

Chapter 6. Future climate changes

6.1 Emission scenarios

6.1.1 The purpose of the scenarios and scenario development

As discussed in Chapter 5, the changes in external **forcing** have to a large extent driven past climate variations. In order to “predict” the climate of the 21st century and beyond, it is thus necessary to estimate future changes in the forcing. This is achieved by the development of **scenarios** for the emission of **greenhouse** gases, **aerosols**, various pollutants in the atmosphere, land use, etc. These **scenarios** depend on many uncertain factors (as discussed below) and some of the uncertainties in the estimates of future climate changes are related to these factors (see Fig. 6.8). This is the reason why, in the scientific literature, the term climate **projection** is generally preferred to the term climate prediction, as it emphasises the fact that the results depend on the **scenarios** chosen and the hypothesis made in those scenarios. The scenarios are also used for analysing impact, adaptation and vulnerability, thus providing a consistent approach for socio-economic and climatic issues.

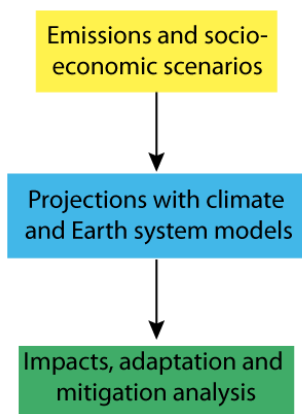
Various types of scenarios have been proposed in recent years and decades. In the fourth assessment report of the IPCC, the climate **projections** were based on the SRES scenarios (Special Report on Emission Scenarios, see Section 6.1.2) which cover the whole of the 21st century. Those scenarios were derived in a sequential form (Fig.6.1). First, the main driving forces influencing the emissions from demographic, social and economic development have to be identified. This implies estimating population growth, future levels of economic activity, the way exchanges between different countries will be organised, the technology choices/opportunities of the countries, etc. On the basis of these estimates, some models produce scenarios for future emissions of greenhouse gases and aerosols, and for land-use changes. Different combinations of demographic and socio-economic change can lead to similar emission paths. For instance, large population growth combined with efficient technologies and renewable energy can lead to similar emissions to a smaller increase in the Earth’s population with less efficient and more energy-demanding technologies. In addition to the emission scenarios, the concentrations of greenhouse gases and aerosols in the atmosphere are also provided for models that do not include a representation of the carbon and/or aerosols cycle.

For the next IPCC assessment report (IPCC AR5), a slightly different approach was followed. Four representative concentration pathways (RCPs) were selected, covering a wide range of future changes in **radiative forcing** (see Section 6.1.3). The emissions (and concentrations) of greenhouse gases corresponding to these four RCPs were then provided to the climate-modelling community, so that they could perform climate **projections**. In parallel, possible socio-economic scenarios compatible with those RCPs were developed, providing different socio-economic alternatives for the same RCP. If needed, the information provided by the climate-model projections can be used in the socio-economic scenarios to assess the impact of climate change on society. Such a parallel approach strengthens the collaboration between the different communities, while ensuring that the climate-modelling groups only have to run a small set of well contrasted emission scenarios with their models (which are very demanding of computer time). Another advantage of the new scenarios is that they include both more detailed short term estimates (to about 2035) and stylised estimates to about 2300, in addition to the classical, long-term estimates up to 2100 provided by the SRES scenarios.

Neither the SRES nor the RCPs made any attempt to provide a best guess or to assess the likelihood of the various scenarios. Many elements of the scenarios are too

unpredictable for this to be feasible. As a consequence, all the scenarios should be considered as reasonable possible and equally probable.

Sequential approach



Parallel approach

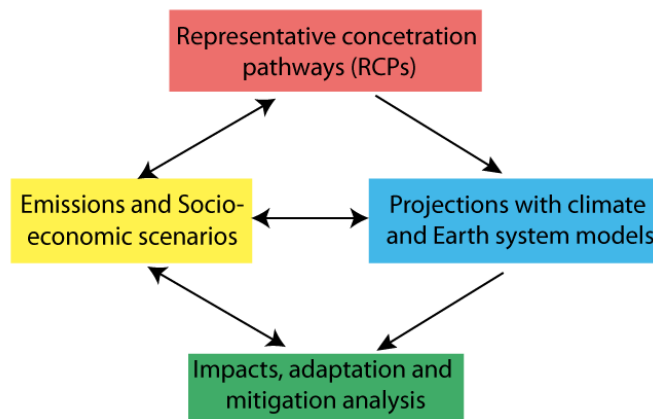


Figure 6.1: Sequential and parallel approaches to the development of scenarios. In contrast to the sequential approach, in the parallel approach the projections with climate models (driven by RCPs) and the choice of emission and socio-economic scenarios (corresponding to those RCPs) are performed concurrently. Modified from Moss et al. (2007).

6.1.2 Special Report on Emission Scenarios (SRES)

Among the infinite number of possible alternative futures, four families have been proposed, comprising 40 SRES scenarios covering a wide range of possibilities. Each family includes a so-called storyline, providing a coherent descriptive narrative of the choices made. The four families can be described very briefly as follows (for more details see Nakicenovic and Swart, 2000):

- + A1 corresponds to very rapid economic growth, low population increase, and the rapid introduction of efficient technologies. The A1 family assumes strong interactions between different countries and a reduction in regional differences in per capita income. In addition, the A1 family is separated into four groups related to technology choices, one group for instance being devoted to fossil-intensive energy production.
- + A2 corresponds to a slow convergence between regions and a high population growth. Technological changes are more slowly implemented than in the other storylines, with more disparity between the regions.
- + B1 corresponds to a low population growth and strong convergence between regions, but with faster introduction of clean and resource-efficient technologies than A1.
- + B2 corresponds to intermediate population and economic growth with less rapid introduction of new technologies than in the B1 and A1 storylines. It assumes an emphasis on local and regional solutions.

6. Future climate changes

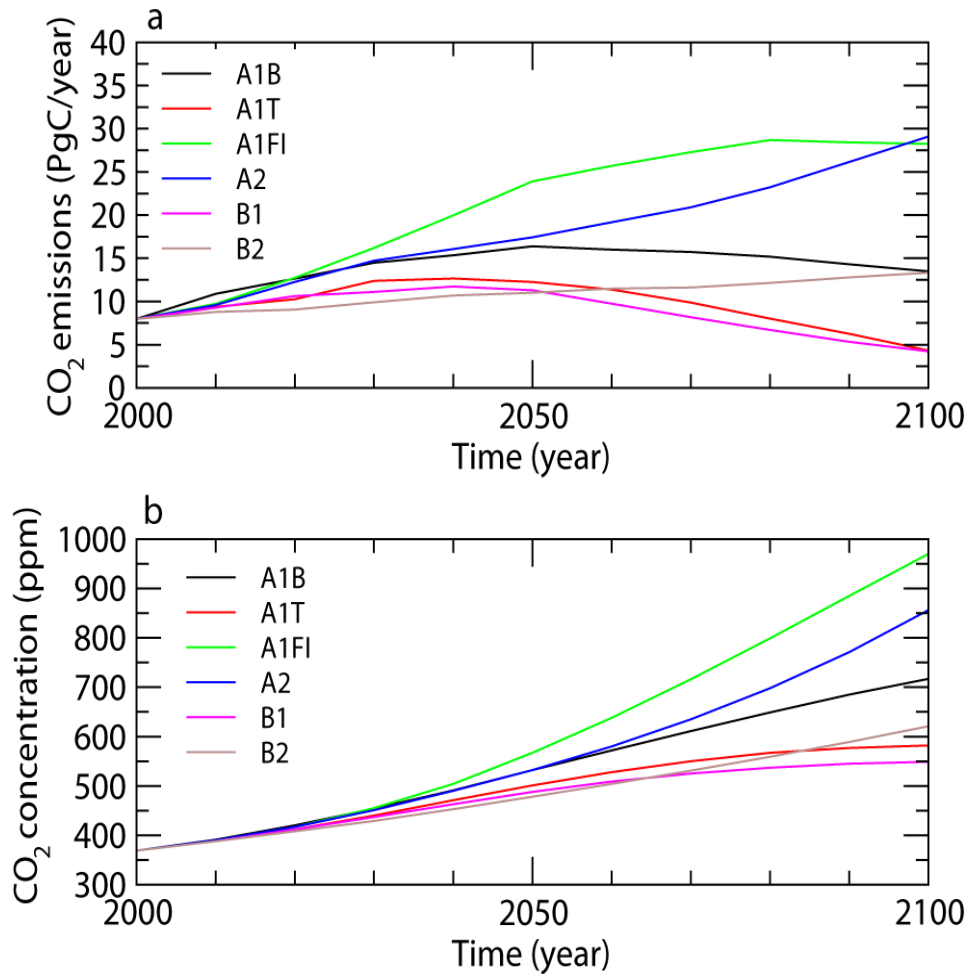


Figure 6.2: (a) Global emission (in PgCO₂ per year) and (b) atmospheric concentration of CO₂ (in ppm) in the 6 illustrative SRES scenarios (A1B, A1T, A1FI, A2, B1, B2).

From those storylines, different research groups have proposed different scenarios. From these, four marker scenarios were selected, one to illustrate each storyline. Two additional scenarios were selected in the A1 family to illustrate alternative developments in energy systems. This resulted in six scenarios, which have been used to perform climate projections (see Section 6.2).

It is important to remember that none of those storylines involves clear climate initiatives or climate-related regulations, although the policy choices described in the various scenarios would have a substantial impact on the emissions of greenhouse gases and aerosols.

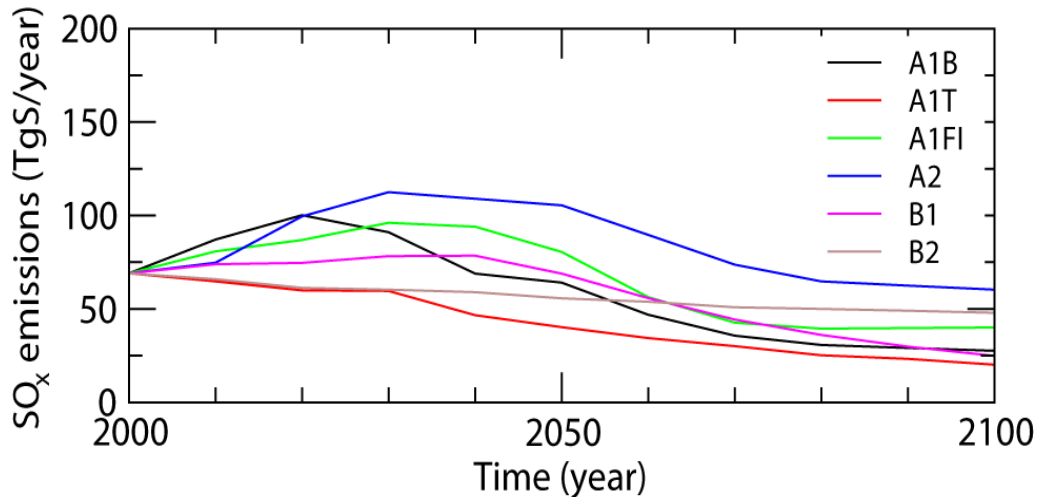


Figure 6.3: Global emissions of sulphur oxides in six illustrative SRES scenarios (in TgS per year).

In all six illustrative scenarios, the emissions of CO_2 increase during the first decades of the 21st century (Fig. 6.2). This trend continues up to 2100 in three scenarios, while the emissions peak between 2030 and 2050 and then decrease in scenarios A1T, B1 and A1B. Based on computations made by the teams that developed the scenarios, this induces an increase in atmospheric CO_2 concentration in 2100 up to nearly 1000 ppm in scenario A1F and a bit less than 600 ppm in scenario B1. This last value roughly corresponds to a doubling of the CO_2 concentration compared to the pre-industrial level (around 280 ppm, see Section 2.3.1). Note that those concentrations were derived using a particular model and some specific hypotheses. A climate model including a carbon-cycle model and thus its own representation of climate/carbon feedbacks, driven by the same SRES emission scenario, will lead to atmospheric CO_2 concentrations different to those plotted in Figure 6.2 (as discussed in Section 6.2.3, below).

SRES scenarios also provide estimates for future emissions and concentrations of other greenhouse gases (such as N_2O and CH_4), as well as emissions of sulphur dioxide (SO_2) which leads to the production of sulphate **aerosols** in the atmosphere. In contrast to CO_2 , SO_2 emissions reach their maximum in all the scenarios during the first half of the 21st century and then decrease (Fig. 6.3) thanks to policies devoted to reducing air pollution. Because of the relatively short life of aerosols in the atmosphere (see Section 4.1.2.2), sulphate concentration changes in roughly the same way over time as the emissions. As a consequence, the negative **radiative forcing** due to aerosols (see Fig. 4.2) will decrease during a large part of the 21st century, while the positive forcing due to greenhouse gases will increase continuously in the majority of the scenarios.

6.1.3 Representative concentration pathways (RCPs)

A set of four RCPs were selected. The most extreme one, RCP8.5 displays a continuous rise in **radiative forcing** during the 21st century, leading to a value of about 8.5 W m^{-2} in 2100. RCP6.0 and RCP4.5 are characterised by a steady rise during the 21st century, up to a **radiative forcing** of about 6 and 4.5 W m^{-2} respectively, and a stabilisation after 2100. Finally, in RCP3-PD (peak and decline), the **radiative forcing** peaks before 2100 at about 3 W m^{-2} and then declines. Emissions and atmospheric concentrations of CO_2 corresponding to those RCPs are shown in Figure 6.4. As expected, CO_2 being the largest contributor to **radiative forcing** (see Fig. 4.2), the time series of atmospheric CO_2 concentration have the same shape as the time series for **radiative forcing**. By construction, the emissions cover a wide range of possibilities,

6. Future climate changes

with, for instance, nearly no emission of CO_2 after 2080 in RCP3-PD while in RCP8.5 the emissions are more than 25 PgC per year (i.e. more than 3 times greater than in 2000).

The RCP also includes estimates of emissions of a large number of greenhouse gases and atmospheric pollutants (CH_4 , N_2O , **chlorofluorocarbons**, SO_2 , black carbon, etc.) as well as estimates of future changes in land use. For instance, in all the RCPs, the decrease in SO_2 emissions (Fig. 6.5) is even larger than in the SRES (Fig. 6.3).

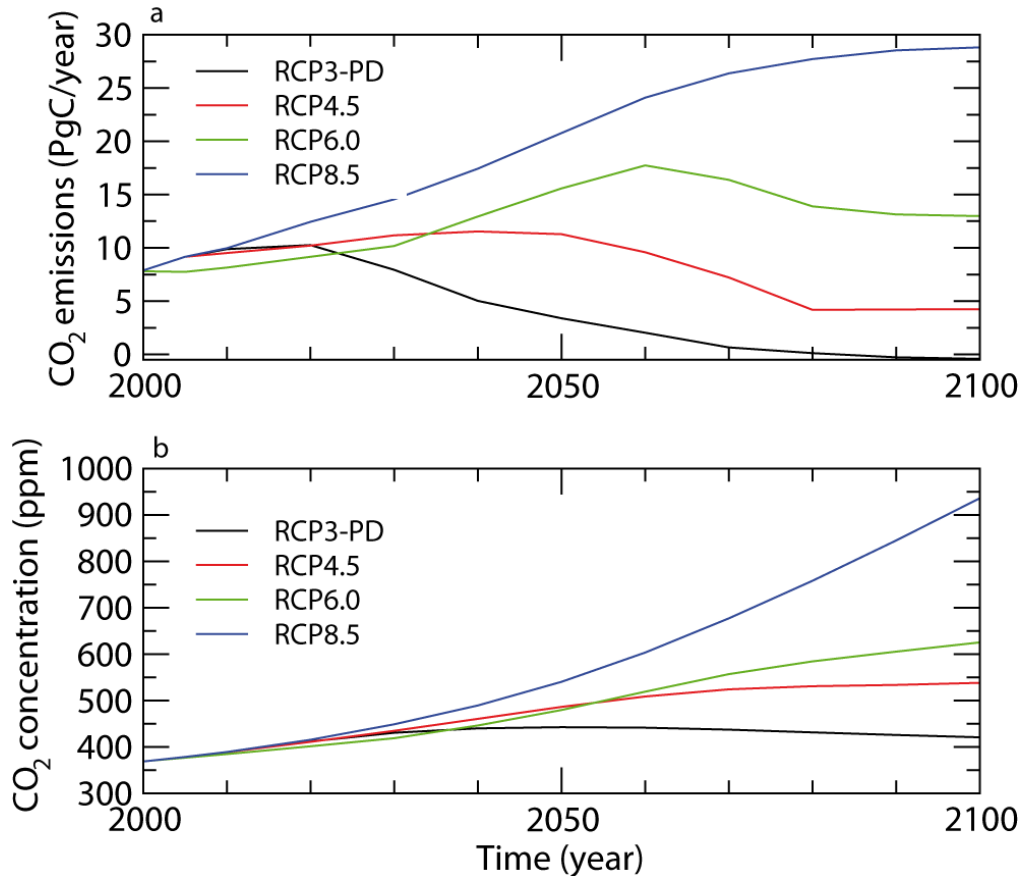


Figure 6.4: (a) Global emission (in PgC per year) and (b) atmospheric concentration of CO_2 (in ppm) in four RCP scenarios.

Furthermore, the RCPs have been extended to 2300 and even 2500 for studies of long-term climate change (Fig. 6.6). Because of the very large uncertainties in the driving forces influencing the emissions, the long-term scenarios are kept as simple as possible and thus highly idealised. Nevertheless, they provide a reasonable range for the possible changes, give time developments compatible with the RCPs over the 21st century, and display a common framework in which the results of different models can be displayed. Among the various possible extrapolations, a forcing stabilisation path emerges for RCP4.5 and RCP6.0. For RCP3-PD, the forcing is assumed to continue to decrease after 2100. For RCP8.5, the extension suggests an increase in forcing until at least 2200, although the emissions growth slows in the second part of the 21st century, leading to a nearly flat profile after 2100.

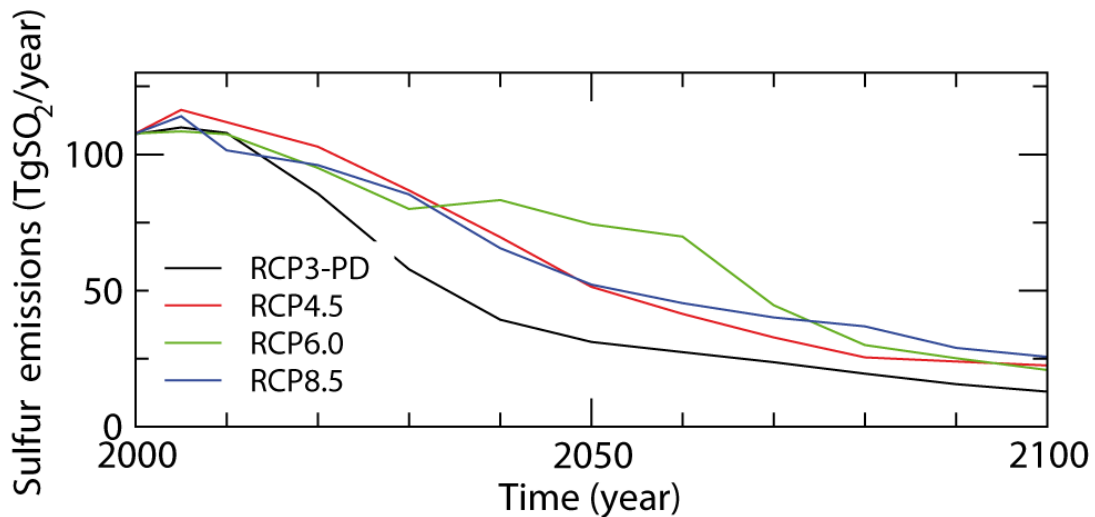


Figure 6.5: Global emissions of sulphur oxide in four RCP scenarios (in TgSO₂ per year).

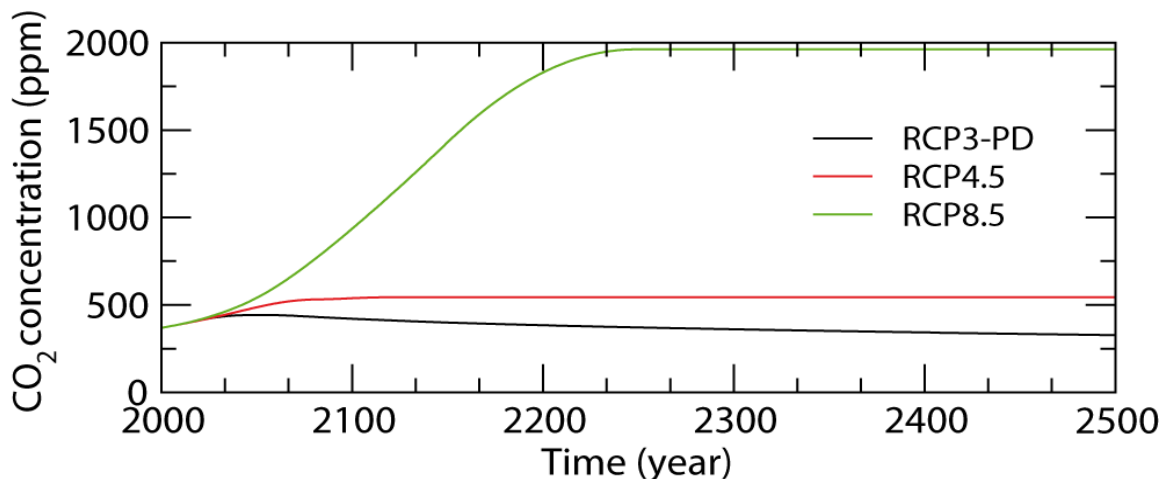


Figure 6.6: Global atmospheric concentration of CO₂ (in ppm) in three RCP scenarios.

6.2 Climate projections for the 21st century

6.2.1 Changes in global mean surface temperature

Nearly all the simulations covering the 21st century available up to now have been obtained using the SRES scenarios (see Section 6.1.2 above). The average of the results of the General Circulation Models (GCMs) is a warming of nearly 2°C by 2100 for scenario B1, a bit less than 3°C for scenario A1B and about 3.5°C for scenario A2 (Fig. 6.7). Fewer models have been driven by the other scenarios, but A1T and B2 generally lead to a forecast warming intermediate between those obtained with scenarios B1 and A2, while scenario A1F1 predicts more warming than A2. An additional scenario that has been widely tested is the so-called constant commitment scenario in which the concentration of greenhouse gases is held constant at year 2000 values for the whole of the 21st century. Even in this extreme case, the GCM simulations predict an average warming of more than 0.5°C by 2100 on average (Fig. 6.7). This is because the climate was far from equilibrium with the forcing in 2000.

6. Future climate changes

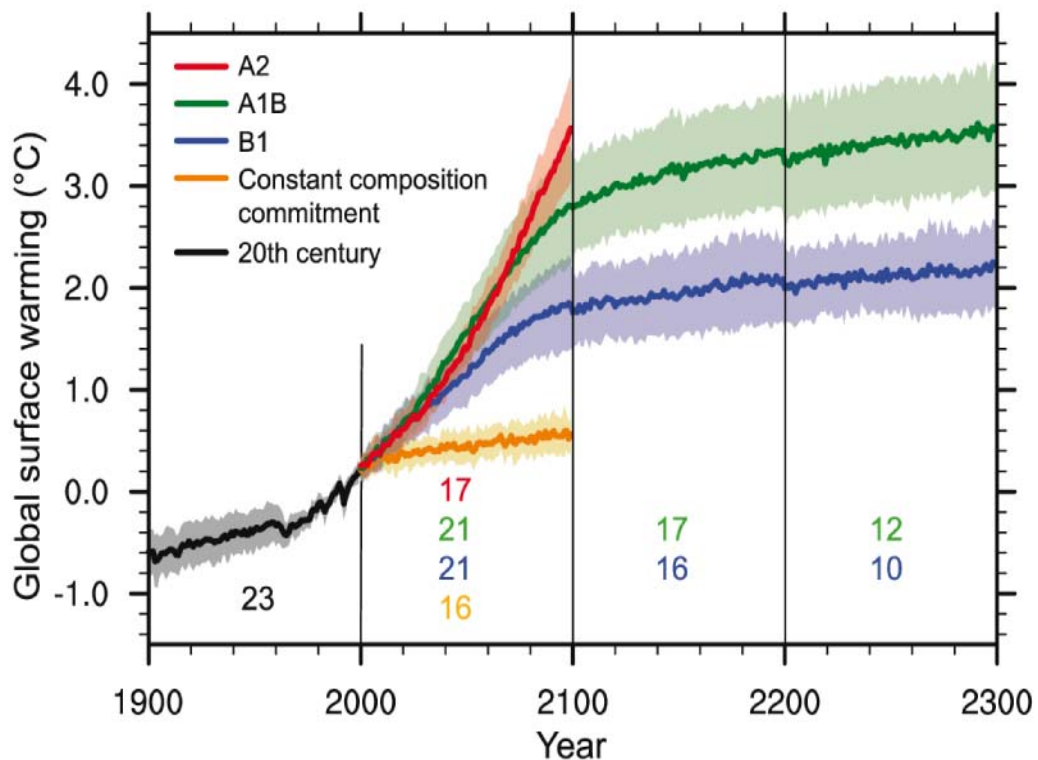


Figure 6.7: Multi-model means of surface warming (relative to 1980-1999) for the SRES scenarios A2, A1B and B1, shown as continuations of the 20th-century simulation. Values beyond 2100 are for the stabilisation scenarios in which the forcing in 2100 is kept constant for the 22nd and 23rd centuries. For the constant composition commitment, the composition in 2000 is maintained during the whole 21st century. Linear trends from the corresponding control runs have been removed from these time series. Lines show the multi-model means, shading denotes the 1 standard deviation range of individual-model annual means. Discontinuities between different periods have no physical meaning and are caused by the fact that the number of models that have run a given scenario is different for each period and scenario, as indicated by the coloured numbers given for each period and scenario at the bottom of the panel. Figure 10.4 of Meehl et al. (2007) with a modified legend, reproduced with permission from IPCC.

Figure 6.7 illustrates two sources of uncertainty in climate projections. The first is related to the scenario, as discussed above. A second is due to model uncertainty, different models displaying a different response to the same forcing. This is indicated on Figure 6.7 by the range of the results of all the models. Additional uncertainty is related to the internal variability of the system, i.e. the natural fluctuations that would occur even in the absence of any change in **radiative** forcing.

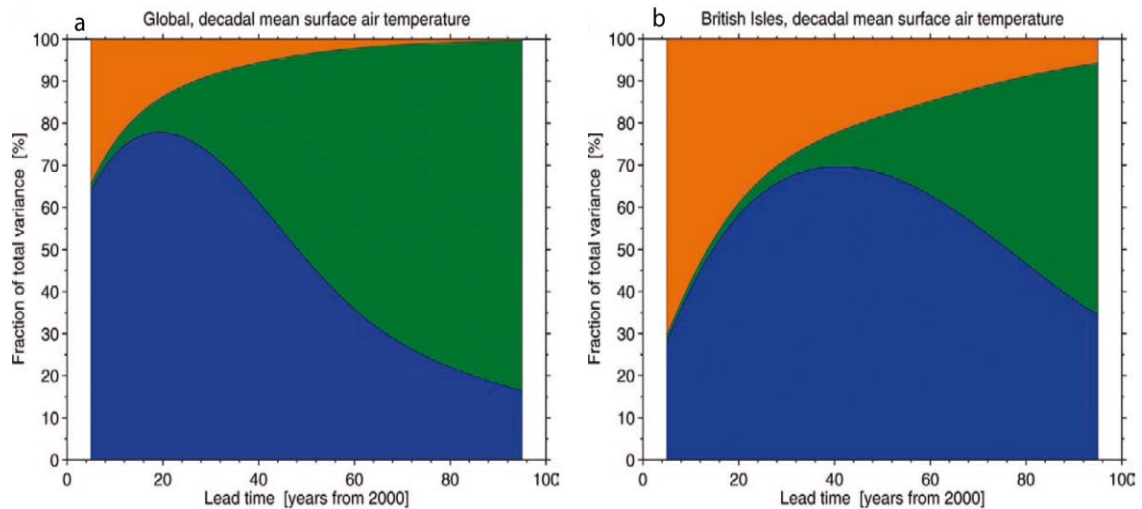


Figure 6.8: The fraction of total variance in decadal mean surface air temperature predictions explained by the three components of total uncertainty is shown for (a) a global mean and (b) a British Isles mean. Green regions represent scenario uncertainty, blue regions represent model uncertainty, and orange regions represent the internal variability component. As the scope of the model is reduced (e.g. from the world to the British Isles), the relative importance of internal variability increases. Figure from Hawkins and Sutton (2009), copyright American Meteorological Society 2009.

The relative importance of the three sources of uncertainty can be estimated for projections over different time periods (also known as lead times). For estimates of the global mean temperature over the next decade, the influence of the uncertainty about future emissions of greenhouse gases is small. This is consistent with Figure 6.7, where the curves for all the SRES scenarios lie close to each other until 2030–2040. On a global scale (Figure 6.8a), the relative importance of the scenario uncertainty increases with time, and is dominant in **projections** for the end of the 21st century. The internal variability only plays a role for a few decades, the natural fluctuations in global mean temperatures over decades and centuries being much smaller than the changes expected by 2100. The model uncertainty is dominant for projections up to 40 years ahead, but its relative contribution then decreases, although it is still significant in 2100.

When analysing temperature changes over a smaller region such as the British Isles (Figure 6.8b), each source of uncertainty has more or less the same behaviour as discussed for the Earth as a whole. The only clear change is that internal variability makes a larger contribution to the total uncertainty. Natural fluctuations also have a much larger amplitude on a regional scale than on the global one (see Section 5.5.2.2).

6.2.2 The spatial distribution of surface temperature and precipitation changes

The increase in global mean temperature by 2100 is associated with a warming in all regions according to the multi-model average (Fig. 6.9). The regional pattern is similar in all the scenarios, with a larger change over the land than over the ocean. This is due to the larger thermal inertia of the ocean and to the increase in latent heat loss that mitigates the temperature changes there. The amplitude of changes is particularly low over the high latitude oceans because of the deeper mixed layer and the contact with colder deep water which has not recently been exposed to surface warming. Additionally, in some models, changes in ocean currents may be responsible for the very small warming, or even a small cooling predicted for the North Atlantic (see Section 6.2.3 below). The changes simulated for the Arctic are also much larger than at mid-latitudes, partly because of the temperature/**albedo** feedback and other feedbacks related to the **cryosphere** (see Section

6. Future climate changes

4.2.3). Changes in heat transport, clouds and the water-vapour feedback also play a role in this behaviour.

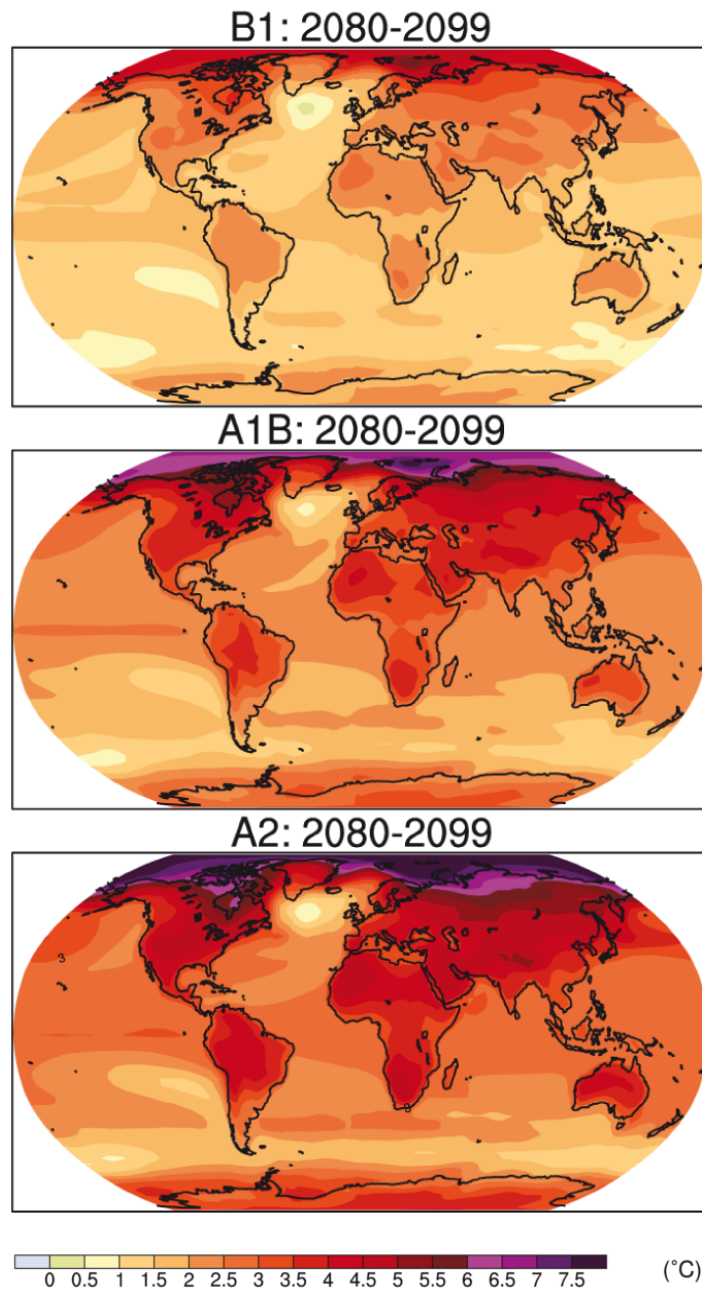


Figure 6.9: Multi-model mean of annual mean surface warming (surface air temperature change, °C) for the scenarios B1 (top), A1B (middle) and A2 (bottom), for the time period 2080 to 2099. Anomalies are relative to the average of the period 1980 to 1999. Modified from Figure 10.8 of Meehl et al. (2007), reproduced with permission from IPCC.

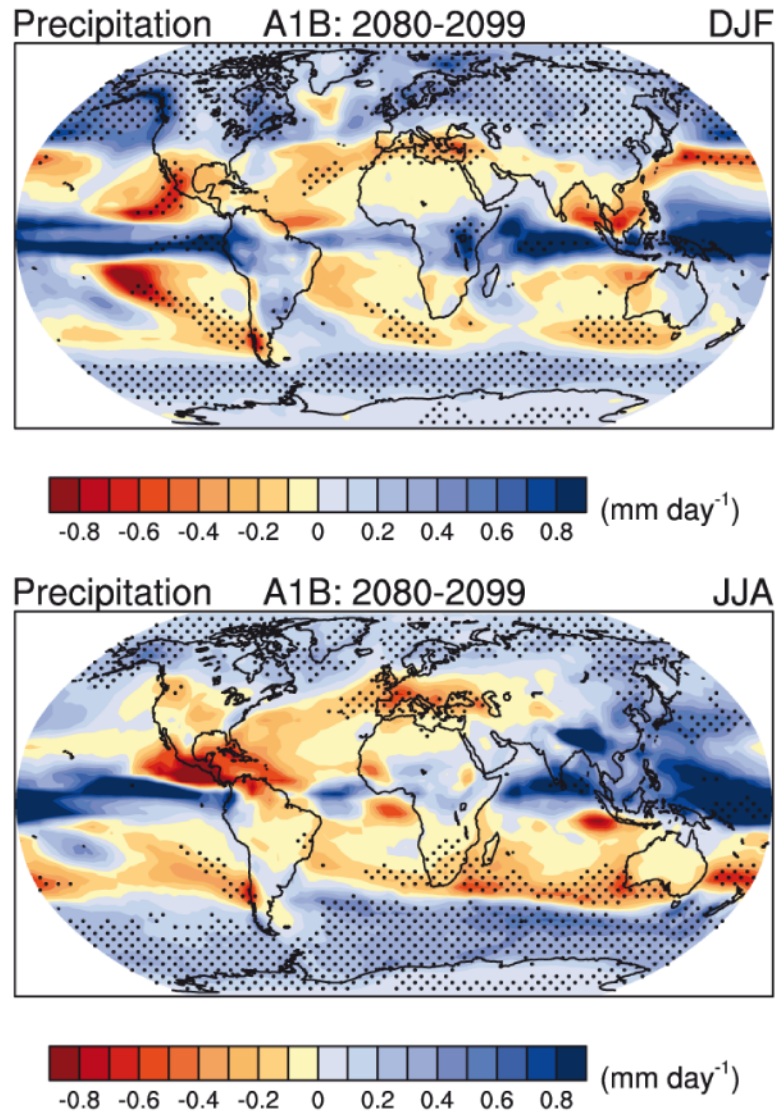


Figure 6.10: Multi-model mean changes in precipitation (mm day^{-1}) for boreal winter (DJF, top) and summer (JJA, bottom). Changes are given for the SRES A1B scenario, for the period 2080 to 2099 relative to 1980 to 1999. Stippling denotes areas where the magnitude of the multi-model ensemble mean exceeds the inter-model standard deviation. Modified from Figure 10.9 of Meehl et al. (2007), reproduced with permission from IPCC.

Global warming is associated with a global increase in precipitation (see Fig. 6.10). This is because of the greater evaporation over the ocean and the larger water-holding capacity of the atmosphere in a warmer world, as described by the **Clausius-Clapeyron equation**. Depending on the model and the scenario, the predicted increase by 2100 is between 1 and 8% compared to the late 20th century. More importantly, this increase in precipitation is far from being spatially uniform and varies strongly over the seasons. At high latitudes, both the multi-model mean and the large majority of individual models predict an increase in precipitation in both winter and summer. An increase in precipitation is also predicted over the tropical oceans, and in the regions influenced by the summer monsoon in South Asia. By contrast, precipitation is predicted to decrease over many subtropical areas and in particular regions such as tropical Central America and the Caribbean, and the Mediterranean.

6. Future climate changes

These changes in the annual and seasonal mean temperature and precipitation are important elements of the projected climate for the 21st century. However, many other characteristics of the atmospheric state, such as wind intensity or cloud amount, are also expected to change. For instance, nearly all the models simulate an increase in the intensity of the westerly winds over the Southern Ocean in the near future, which can also be related to an increase in the Southern Annular Mode (SAM) index (see Section 5.2.3). A particularly sensitive point is the change in the probability of extreme events (such as major storms and heat waves) in a warmer climate. Such extreme events are difficult to model and the available time series are usually too short for reliable predictions to be made for rare events. However, some simple arguments suggest that even a small change in the mean temperature greatly increases, for example, the probability of experiencing a temperature above a particular threshold, and thus of an increase in the number of very hot days (Fig. 6.11). A rise in average temperature also decreases the probability of the temperature falling below a particular level, and so decreases the probability of cold days. This simple reasoning is in agreement with model results which suggest an increase in heat waves in summer and a decline in the incidence of frosts in many regions.

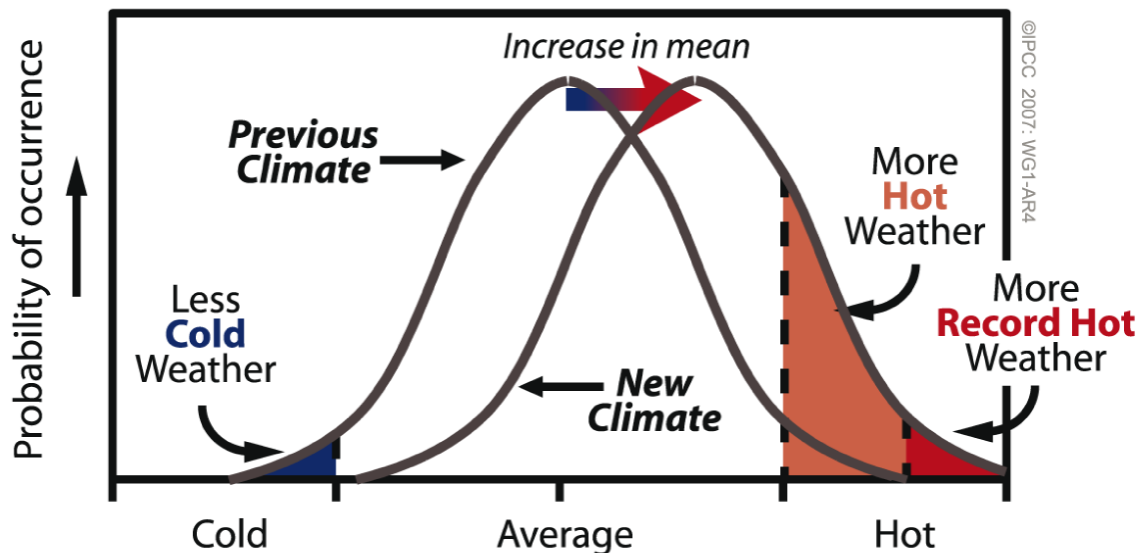


Figure 6.11 Schematic diagram showing the effect of mean temperature increases on extreme temperatures, for a normal temperature distribution. Figure 1, Box TS5 of Solomon et al. (2007). Reproduced with permission of IPCC.

Fig. 6.11 is based on a simple shift in the distribution but the shape of the distribution can also change. Indeed, some studies suggest that the future climate will also be more variable in some regions (corresponding to a wider distribution on Fig. 6.11 and thus even more frequent extremes), although those results are not always robust between the different models.

6.2.3 Changes in the ocean and sea ice

The warming simulated at high latitudes is associated with year-long decreases in the extent and in the thickness of sea ice in both hemispheres. The projected decrease is larger in summer than in winter, and particularly pronounced in the Arctic. As a consequence, both hemispheres are predicted to move towards seasonal ice cover during the 21st century. The differences between the projections provided by the various models are quite large and so are the uncertainties, but many simulations forecast a totally ice-

free Arctic in summer before the end of the 21st century, although some ice would still be present in winter (Fig. 6.12).

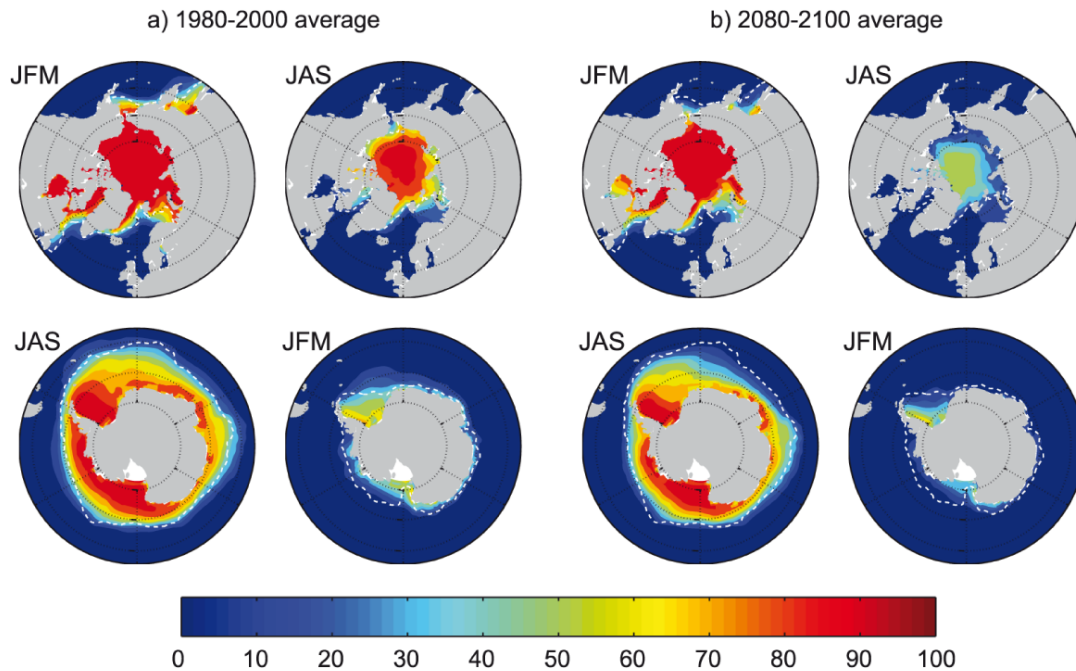


Figure 6.12: Multi-model mean sea ice concentration (%) for January to March (JFM) and June to September (JAS), in the Arctic (top) and Antarctic (bottom) for the periods (a) 1980 to 2000 and b) 2080 to 2100 for the SRES A1B scenario. The dashed white line indicates the present-day 15% average sea ice concentration limit. Figure 10.14 of Meehl et al. (2007), reproduced with permission from IPCC.

Ocean circulation is also projected to change during the 21st century. Because of the warming and the increase in precipitation at high latitudes (see Section 6.2.2), the density of the water at the surface will tend to decrease, increasing the stratification in many regions. In the North Atlantic, this would imply less sinking of dense water and a weaker southward transport of dense water. As a consequence, the northward transport of warm surface water will also decrease with potential implications for the heat budget of the North Atlantic and the surrounding regions.

The intensity of this **thermohaline circulation** is generally measured by the maximum of the **meridional overturning circulation** (MOC) in the North Atlantic, although the two concepts are slightly different (the overturning circulation also including the contribution from the winds). The scatter of the results for the thermohaline circulation from the different GCMs is very large, both for present-day conditions and for the whole 21st century (Fig. 6.13). Three simulations show a clear slow down during the 20th century. This is not related to the forcing during this period, but rather to a slow drift of the model to a state that is inconsistent with observational estimates. All the other models have more realistic predictions for the 20th century, with the meridional overturning circulation ranging from a more or less stable situation over the 21st century to decreases of more than 50% compared to the late 20th century. None of them simulates a complete collapse of the circulation, a state which is sometimes referred to as the off-state of the meridional overturning circulation.

6. Future climate changes

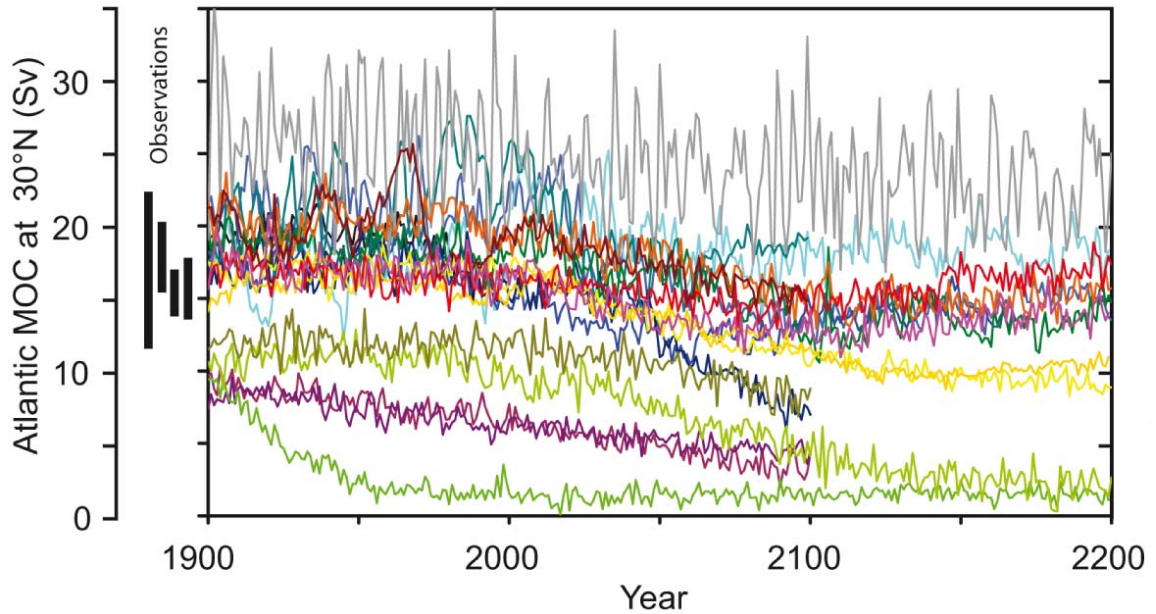


Figure 6.13 The changes in the Atlantic **meridional overturning circulation** (MOC) at 30°N in simulations with several coupled climate models from 1850 to 2100 using the SRES A1B emissions scenario for 1999 to 2100 (in $\text{Sv} = 10^6 \text{ m}^3 \text{ s}^{-1}$). Some of the models continue the integration to year 2200 with the forcing held constant at the values of year 2100. Observationally based estimates of late-20th century MOC are shown as vertical bars on the left. Modified from Figure 10.15 of Meehl et al. (2007), reproduced with permission from IPCC

6.2.4 Changes in the carbon cycle and climate-carbon feedbacks

In the previous two sections, we have briefly described the influence of anthropogenic forcing on climate. In turns, climate changes have impacts on the biogeochemical cycles, leading to modifications of the **radiative forcing** with potential feedback effects on climate. Among all the complex mechanisms involved, we will focus here on CO_2 as it is the dominant anthropogenic gas (see Section 4.1.2.1).

As mentioned in Section 2.3.1, about half of the anthropogenic CO_2 emitted by fossil-fuel burning and changes in land use has stayed in the atmosphere. The remaining half is stored approximately equally in the ocean and terrestrial biosphere. However, this division of anthropogenic emissions between atmospheric, oceanic and land reservoirs will change in the future.

First, the changes in atmospheric CO_2 concentration itself modify the atmosphere-ocean and atmosphere/land CO_2 fluxes. The balance between H_2CO_3 , HCO_3^- and carbonate ions CO_3^{2-} explains why the ocean is able to store large amounts of CO_2 . (see section 2.3.2.1). In particular, the CO_2 which is transferred from the atmosphere reacts with the water to form H_2CO_3 and with carbonate ions (CO_3^{2-}) to obtain bicarbonate ions (HCO_3^-), the dominant form of inorganic carbon in the ocean:



The CO_2 flux from the atmosphere to the ocean during the 20th and 21st centuries will tend to decrease the availability of carbonates ions (at least on time scales from decades to centuries, see Section 6.3.1). This will reduce the efficiency of reaction (6.1)

to form bicarbonates from CO_2 . A larger fraction of the **dissolved inorganic carbon** (*DIC*) will remain as H_2CO_3 , increasing the partial pressure of carbon dioxide in the ocean and thus reduce the oceanic uptake (see Eq. 2.38). As a consequence, the ocean will continue to store some anthropogenic CO_2 , but its relative contribution will decrease.

Over land, the increase of CO_2 concentration in the atmosphere generally implies more assimilation and sequestration of carbon by the terrestrial biosphere through photosynthesis (see Equation 2.46). This CO_2 fertilisation effect is not related to any limitation of plant productivity by CO_2 availability in present-day conditions, but rather to the predicted better regulation of the plant/atmosphere gas exchanges through **stomata** in future. With high levels of CO_2 , smaller exchanges are required for the same CO_2 uptake, implying less transpiration and thus an increase in plants' efficiency of water use. However, many factors limit plant growth, including the availability of nutrients. The long term and large-scale effect of the CO_2 fertilisation effect have not yet been precisely assessed.

These biogeochemical effects (also referred to as concentration effects) will occur even in the absence of any climate change induced by changes in the atmospheric composition. Global warming will also reduce the oceanic solubility of CO_2 (see Section 2.3.2.1). This is one example of a positive climate-carbon cycle feedback. In addition, increased stratification and slower oceanic circulation (see Section 6.2.3) are expected to reduce the exchanges between the surface layers rich in anthropogenic carbon and the deeper layer. The deeper water does not yet contain a significant amount of anthropogenic carbon because of the relatively slow oceanic overturning and diffusion rates (see Section 1.3.2), so the slower renewal of surface waters will tend to induce higher levels of *DIC* at the surface and thus reduce the oceanic uptake of carbon, providing another positive climate/carbon feedback. Changes in marine **biota** could also lead to some feedback loops, but they are not currently well understood. Present-day models suggest that their role is relatively unimportant, but the modelling of marine ecosystems is still very simple, and more precise estimates of those effects are required.

Temperature and precipitation changes also affect the carbon cycle on land. Warming tends to accelerate decomposition in soils, which releases CO_2 to the atmosphere. The primary production is enhanced by warming in cold areas and by an increase in precipitation in dry areas. In addition, in warm, dry areas where water availability is a limiting factor, a decrease in precipitation produces a reduction in productivity and thus in the uptake of CO_2 by vegetation. In addition, climate changes influence the distribution of biomes (see, for instance, Section 4.3.3) as well as the frequency and extent of wildfires (savannah and forest fires) which emit substantial quantities of CO_2 . This illustrates that both positive and negative carbon/climate feedbacks are expected over land in different regions.

In order to estimate the influence of the feedback between climate changes and the carbon cycle, simulations have been performed with climate models including a representation of the carbon cycle (Friedlingstein et al., 2006). In the first group of numerical experiments, both the carbon cycle and the climate were allowed to change in response to anthropogenic CO_2 emissions (SRES A2 scenario). In the second group, the models were again driven by CO_2 emissions, but the climate was kept constant. In other words, the increase in CO_2 was not associated with any change in the **radiative forcing**. Because of this constant climate, the climate/carbon feedback loops were inactive, and it was thus possible in this idealised set-up to measure the contribution of biological processes (the concentration effects) to the changes in the carbon cycle. By studying the difference between the two groups of models, it was then possible to make a first-order estimate of the influence of the carbon/climate feedback loops.

6. Future climate changes

In the fully coupled experiments, where climate and the carbon cycle interact, the concentration of atmospheric CO_2 is predicted to be between 20 and 220 ppm higher than in the constant-climate system by 2100 (Fig. 6.14). The net climate/carbon feedback effect is positive for all the models. This clearly indicates that the modifications in climate mean that a larger fraction of anthropogenic CO_2 will remain in the atmosphere in the future. The models suggest that this is mainly due to the terrestrial biosphere, which will display changes in primary productivity and increased soil respiration in future.

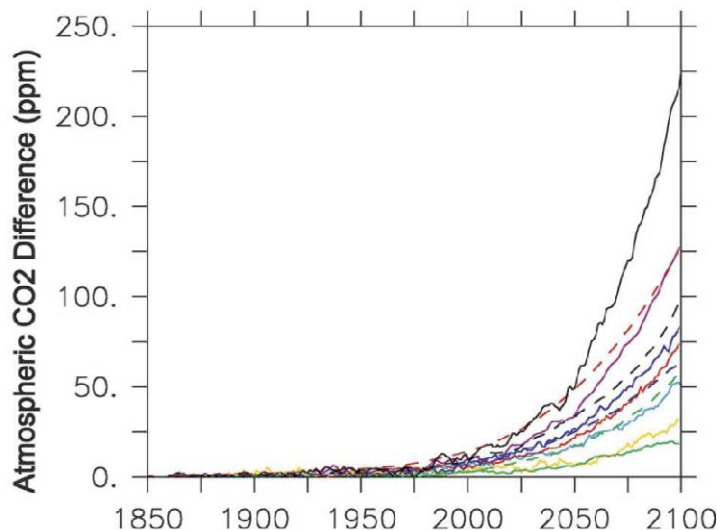


Figure 6.14: Difference between the atmospheric CO_2 predicted by different models of the coupled and uncoupled carbon cycles (ppm) (Friedlingstein et al. 2006). Copyright AMS 2006.

The projections made by models including a carbon cycle driven by emissions of CO_2 can be compared to those directly driven by CO_2 concentrations (Fig. 6.15). It must be recalled here that the concentrations in the SRES scenarios (Section 6.1.2) were obtained using a carbon-cycle model that includes its own representation of climate/carbon feedbacks. Consequently, Figure 6.15 does not display the results of simulations with and without climate/carbon feedbacks, but rather illustrates the impact of different representations of those feedbacks. A first important feature is the large increase in the range of projections in the simulations including carbon-cycle models. Changes in the carbon cycle are thus a key source of uncertainty in climate projections. Second, in the majority of the cases, the projected temperature changes in 2100 are larger in the coupled climate/carbon cycle models, leading to a range of temperature increases of 2.3–5.6°C for Scenario A2.

Another consequence of the flux of anthropogenic carbon from the atmosphere to the ocean is oceanic acidification (see Eqs. 2.39 to 2.41). Over the period 1750–1994, the surface **pH** of the global ocean decreased by about 0.1. The expected decrease by 2100 is about 0.3–0.4 for a standard scenario, the precise value depending on the level of CO_2 emissions. By the year 3000, the decrease may be as high as 0.7. This would lead to **pH** values lower than those estimated for the last few hundred million years.

This ocean acidification increases the solubility of $CaCO_3$, (see Section 4.3.1); this could also be related to the reduced CO_3^{2-} concentration due to oceanic uptake of CO_2 . This will have a clear impact on $CaCO_3$ production by corals as well as by calcifying phytoplankton and zooplankton, and thus on their life cycles (see Section 2.3.2.2). The **aragonite** produced by, for instance, corals, will be particularly influenced by this change as it is less stable than **calcite**.

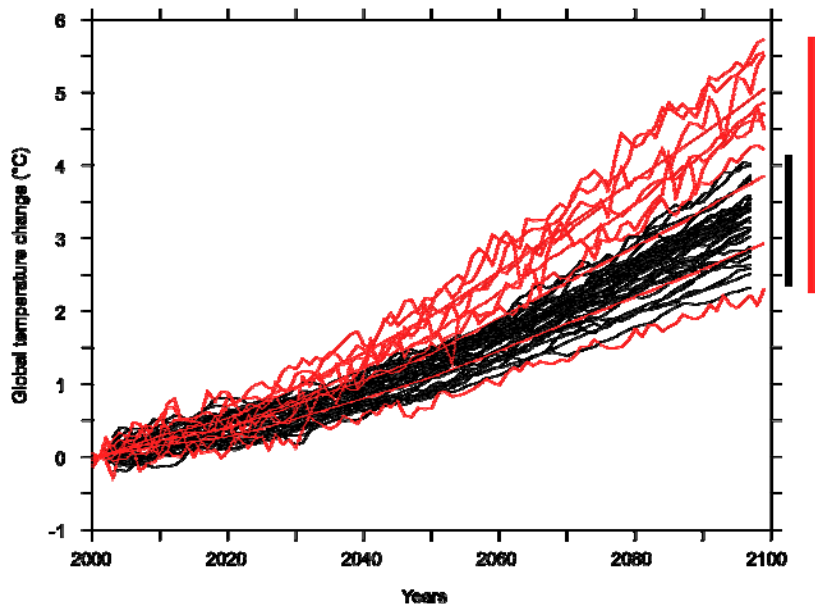


Figure 6.15: Globally averaged surface temperature change (relative to 2000) derived from the coupled climate-carbon cycle models (red) compared to simulations performed with climate models driven by CO_2 , other greenhouse gas and anthropogenic aerosols concentrations (black, as in Section 6.2.1). (Cadule et al. 2009). Copyright AGU 2009.

6.3 Long-term climate changes

6.3.1 The carbon cycle

The interactions between the atmosphere, the land biosphere and the ocean surface layer take place relatively rapidly, and are predicted to play a dominant role in the changes in atmospheric CO_2 concentration over the 21st century (see Section 6.2.4). By contrast, the exchanges of CO_2 with the deep ocean are much slower, taking place on timescales from centuries to millennia. Consider, for instance, a strongly idealised scenario in which CO_2 emissions follow a pathway that would lead to a long-term stabilisation at a level of 750 ppm but, before reaching this level, the emissions were abruptly reduced to zero in 2100. The goal here is not to provide a realistic projection but to analyse the long-term changes in the system after all emissions cease. Figure 6.7 includes an estimate of the warming during the 21st century if the CO_2 concentrations were stabilised at the 2000 level; here, Figure 6.16 shows the changes in CO_2 and surface temperature which will still take place even if there are no additional emissions after 2100.

In all the models driven by this scenario, atmospheric CO_2 concentration decreases after 2100. The deep ocean is not in equilibrium with the surface in 2100, and so carbon uptake by the deep ocean continues during the whole of the third millennium. Depending on the model, the concentrations reached by the year 3000 are between 400 and 500 ppm, i.e. much higher than the pre-industrial level.

Despite this decrease in the CO_2 concentration, the global mean surface temperature is more or less stable during the third millennium, with the majority of models predicting only a slight cooling. The **radiative** forcing due to CO_2 decreases after 2100 but the heat uptake by the ocean also decreases (see Section 4.1.4) as the ocean warms. The two effects nearly balance each other, leading to the simulated stabilisation of temperature.

6. Future climate changes

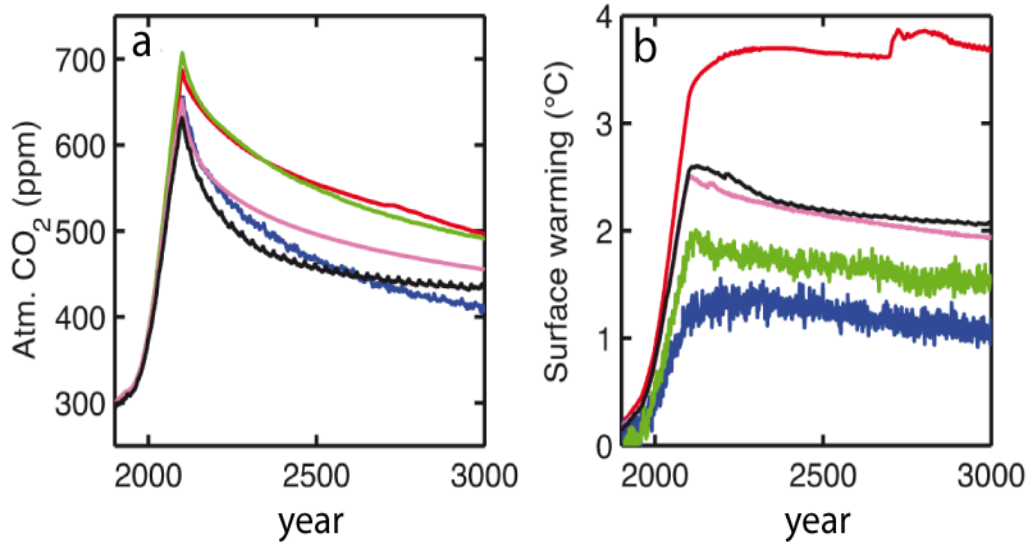


Figure 6.16: Changes in (a) atmospheric CO_2 and (b) global mean surface temperature relative to the pre-industrial period simulated by five intermediate-complexity models for a scenario where the emissions follow a pathway leading to stabilisation of the atmospheric CO_2 at 750 ppm, but, before reaching this target, the emissions are reduced to zero in the year 2100. Modified from Figure 10.35 of Meehl et al. (2007), reproduced with permission from IPCC.

The results displayed in Figure 6.16 mainly deal with the long-term adjustment between the ocean and the atmosphere. However, on long timescales, the changes in acidity caused by the oceanic uptake of CO_2 induce dissolution of some of the $CaCO_3$ in the sediments (carbonate compensation, see Section 4.3.1), modifying the ocean **alkalinity** and allowing an additional uptake of atmospheric CO_2 . Those processes are neglected in the models used in Figure 6.16. If they are included, the interaction with $CaCO_3$ in the sediments increases the ability of the ocean to store CO_2 , producing a further reduction of the atmospheric concentration. However, this process is very slow and after 10,000 years, the atmospheric CO_2 concentration is still predicted to be significantly higher than in pre-industrial times (Fig. 6.17). Even after several tens of thousands of years, the atmospheric CO_2 will not return to pre-industrial levels through this mechanism. On even longer timescales, this will be achieved by the reactions of CO_2 with some rocks, and in particular by the negative feedback caused by weathering (see Section 4.3.2). Because of this long term perturbation of the carbon cycle, the temperature remains significantly higher than in pre-industrial times during the whole period investigated in Figure 6.17, the amplitude of the temperature rise over several millennia being related to the release of carbon at the end of the second and the beginning of the third millennia.

This section illustrates that, because of the wide variety of processes involved, we cannot reliably estimate the timescale for the response of atmospheric CO_2 concentration to fossil fuel burning, as we could for other anthropogenic **forcings** (Figure 4.2). To give an accurate representation of the time changes of atmospheric CO_2 concentration, several different timescales, corresponding to the dominant mechanisms, are required

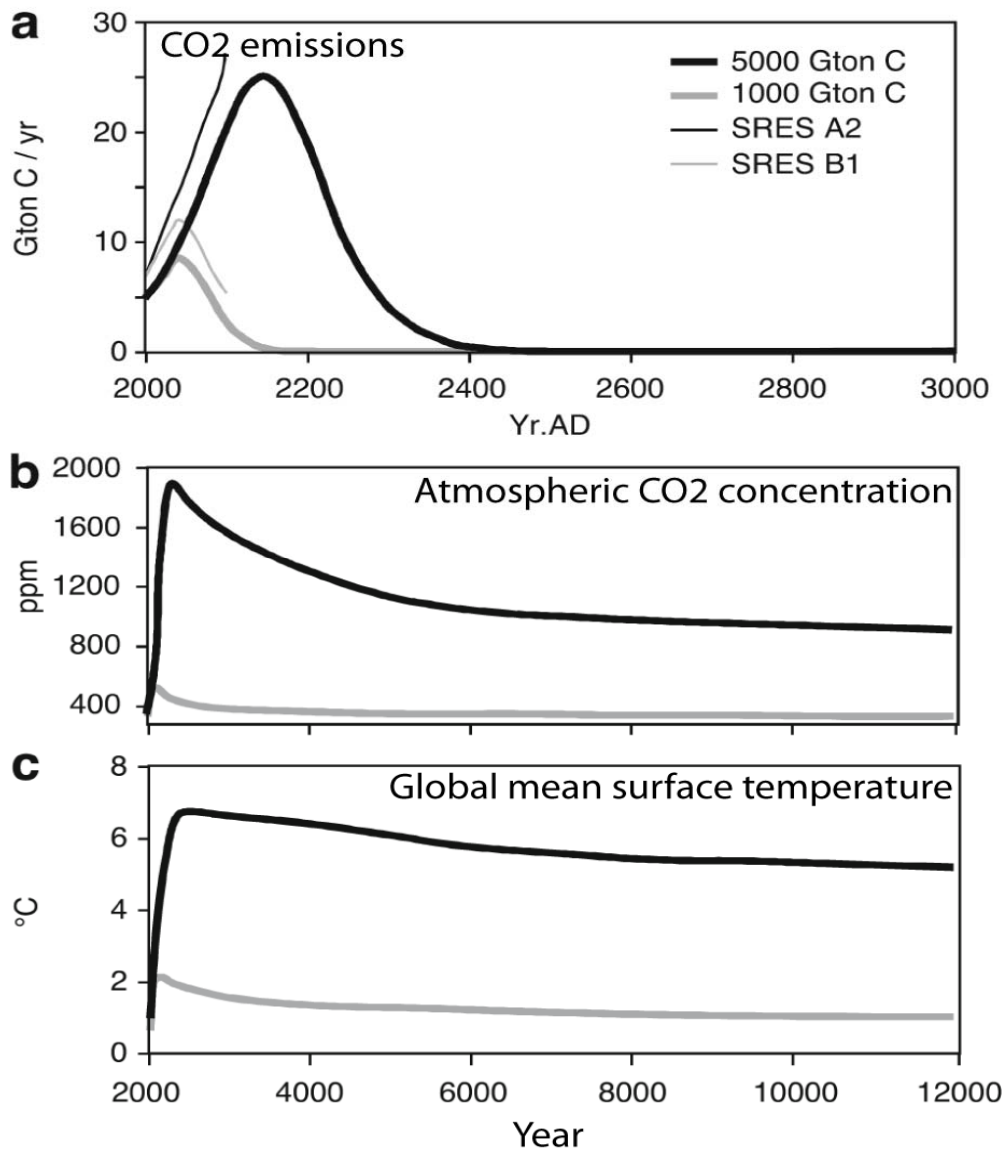


Figure 6.17: The response of the climate model of intermediate complexity CLIMBER-2 to moderate (1,000 Gton C) and large (5,000 Gton C) total fossil fuel emissions. The equilibrium climate sensitivity of the model is 2.6°C. The land carbon cycle was neglected in these simulations while deep sea sediments were explicitly simulated using a sediment model. (a) Emissions scenarios and reference IPCC SRES scenarios (B1 and A2, see Fig. 6.2). (b) Simulated atmospheric CO₂ (ppm). (c) Simulated changes in global annual mean air surface temperature (°C). Figure from Archer and Brovkin (2008). Copyright Archer and Brovkin (2008).

6.3.2 Sea level and ice sheets

Sea levels have changed for two main reasons in recent decades (Fig. 6.18). First water has been added to the ocean from other reservoirs. The main contributors are the glaciers and ice caps that have experienced considerable mass losses during the 20th century because of the large-scale surface warming observed over this period (see Section 5.5.3). The melt water flow from Greenland and Antarctica is relatively small on this time scale, and it is not even clear whether the net flow from the Antarctic is positive or negative.

6. Future climate changes

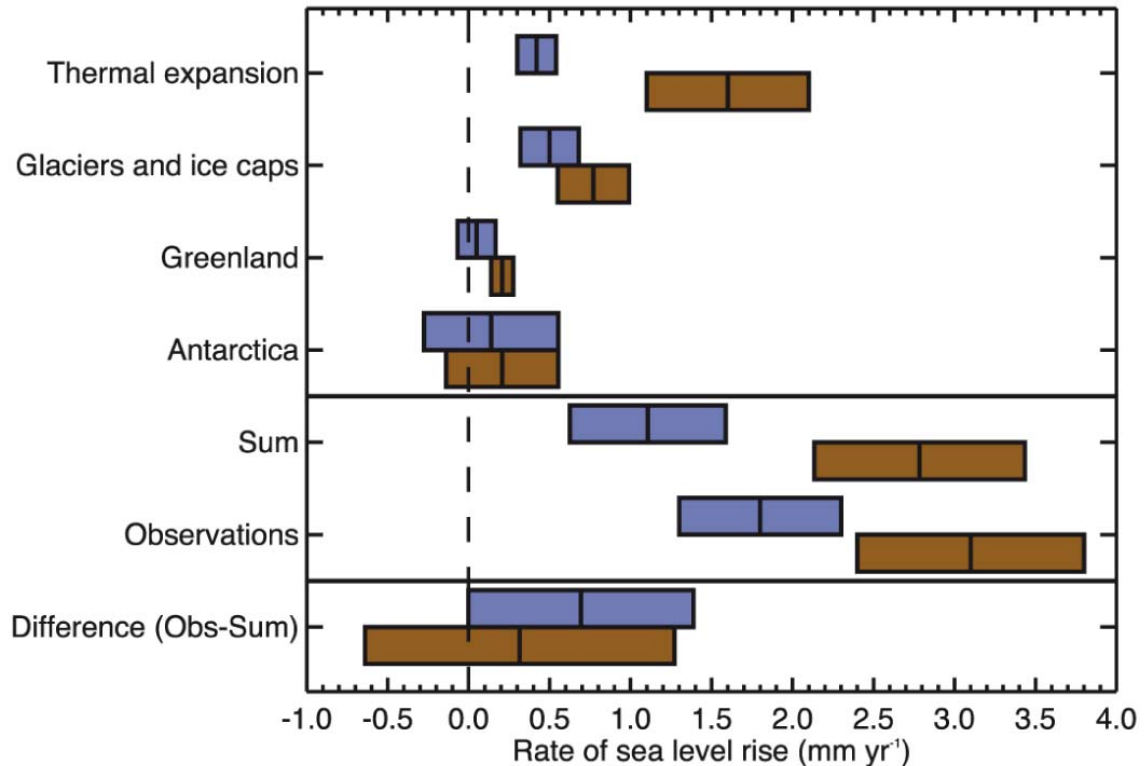


Figure 6.18: Estimates of the various contributions to the budget of the global mean sea level change (upper four entries), the sum of these contributions and the observed rate of rise (middle two), and the observed rate minus the sum of contributions (lower), all for 1961 to 2003 (blue) and 1993 to 2003 (brown). The bars represent the 90% error range. For the sum, the error has been calculated as the square root of the sum of squared errors of the contributions. Likewise the errors of the sum and the observed rate have been combined to obtain the error for the difference. Figure 5.21 of Binoff et al. (2007) with a modified legend, reproduced with permission from IPCC.

The second cause of sea level change is related to the ocean density. For a constant oceanic mass, any modification of the density affects the ocean volume and thus the sea level. As the density variations are mainly ruled by the water temperature, this term is often referred to as **thermal expansion**, although salinity changes can play a non negligible role in some regions. The contribution of this process is similar to that of glaciers and ice caps over the period 1961-2003 but it is clearly the largest contributor if the analysis is restricted to the period 1993-2003. However, this is maybe related to decadal climate variability (Fig. 6.18). Overall, the sea level rise has been estimated at about 1.8 mm yr^{-1} over the period 1961-2003. This is not very different from estimates for the first half of the 20th century but much less than those for the years 1993-2003. Integrated over the whole 20th century, the total sea level rise is then a bit less than 20 cm.

Over the 21st century, the melting of glaciers and ice caps and thermal expansion are expected to remain the two main causes of rising sea levels. Greenland will likely make a small positive contribution. However some frozen water may accumulate over Antarctica, the additional precipitation over a large area of the continent, related to warming (see Section 6.2.3), being approximately equal to the additional melting close to the shore. Indeed, temperatures in the centre of Antarctica are so low that the warming estimated for the 21st century is far too small to produce melting there.

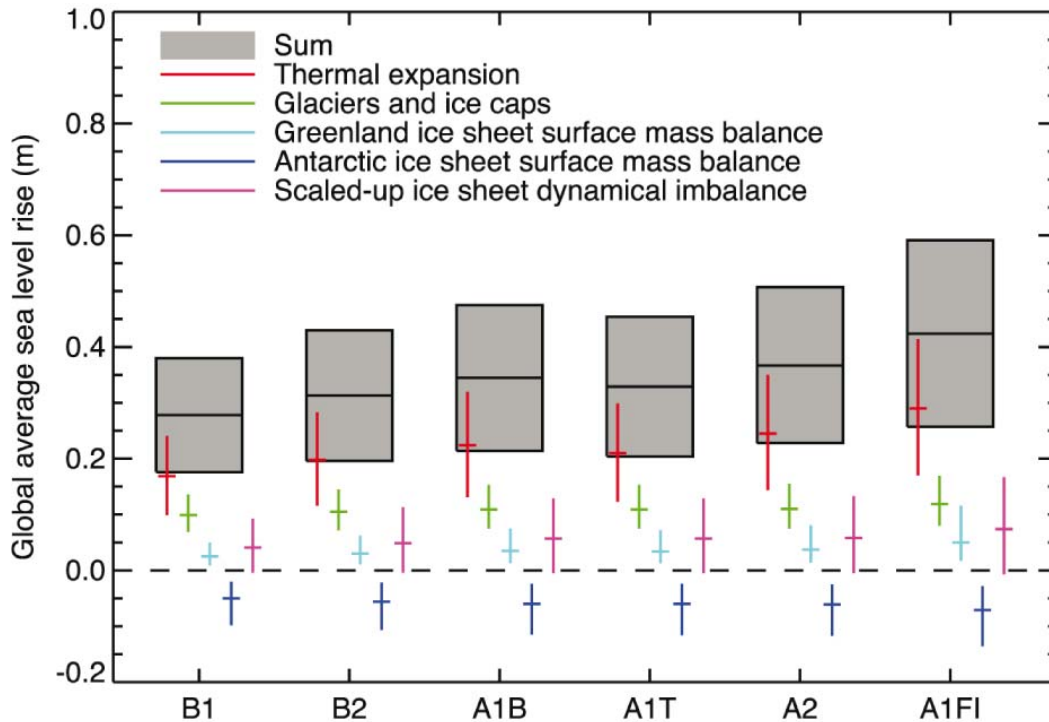


Figure 6.19: Projections and uncertainties (5 to 95% ranges) of global average sea level rise and its components in 2090 to 2099 (relative to 1980 to 1999) for the six SRES marker scenarios. The projected sea level rise assumes that the part of the present-day ice sheet mass imbalance that is due to recent ice flow acceleration will persist unchanged. Figure 10.33 of Meehl et al. (2007) with a modified legend, reproduced with permission from IPCC.

Depending on the scenario, the estimates of sea levels at the end of the 21st century range from 20 to 60 cm higher than in the late 20th century in the latest IPCC report (Figure 6.19). However, many uncertainties remain. The ice-sheet models used to obtain these estimates (see Section 3.3.6) do not include an adequate representation of the rapid ice flow changes that occur on relatively small scales (a kilometre or even less, to a few hundreds of metres), which may transport ice to the ocean or to warmer areas where it would melt relatively quickly. These fast ice-flow changes may be high frequency fluctuations that average out when looking at changes over a century or more. However, it has also been hypothesised that they could induce large-scale destabilisation of parts of the ice sheets, with potentially large consequences for the mass balance of the ice sheet and thus for sea-level rises. As a consequence, alternative methods have been proposed, based on simple statistical relationships between the rises in surface temperatures and sea levels. These studies predict that sea-level rises ranging from 75 to 190 cm by the end of the 21st century are not unlikely (e.g., Vermeer and Rahmstorf, 2009).

Even if the concentration of atmospheric CO_2 stabilises or decreases after 2100, sea levels are predicted to continue to rise fast (see Figure 6.16). First, the deep ocean will have to come into equilibrium with the new surface conditions, leading to warming at deeper levels, and thus thermal expansion over several centuries (Fig. 6.20).

6. Future climate changes

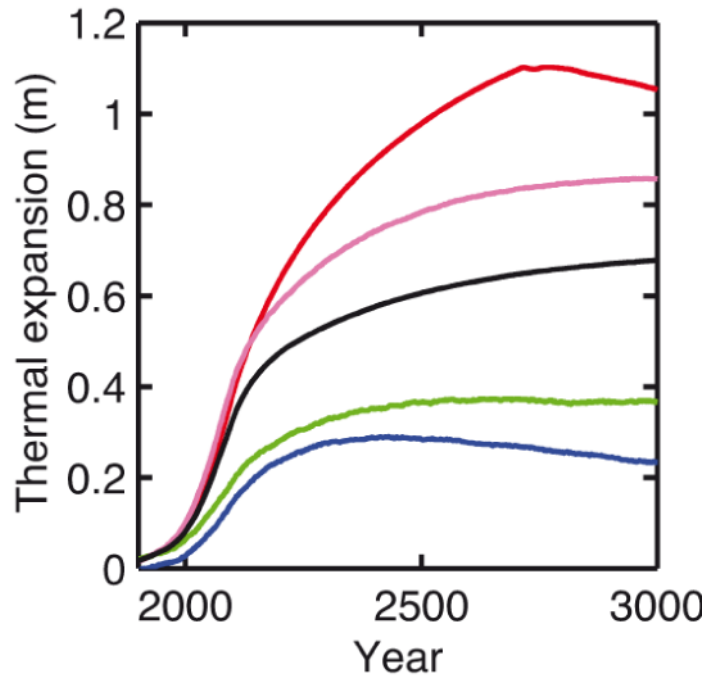


Figure 6.20: Changes in sea level (relative to the pre-industrial period) caused by thermal expansion, as simulated by the same five intermediate-complexity models as in Figure 6.16, for a scenario where emissions follow a pathway leading to stabilisation of atmospheric CO_2 at 750 ppm, but before reaching this target, emissions are reduced to zero instantly at year 2100. Modified from Figure 10.35 of Meehl et al. (2007), reproduced with permission from IPCC.

Second, the thermal inertia of the ice sheets is very large, taking several millennia to tens of millennia to completely melt, even when the warming is considerable. For Greenland, it has been estimated that a sustained local warming of the order of 3–6°C, which is not incompatible with the values provided by models of several scenarios, may be sufficient to induce a complete melting of the ice sheet. The ice sheet would start to melt on its periphery, and would gradually retreat to the centre of the island, to finally survive only in the eastern mountains (see Figure 6.21). As the Greenland ice sheet retreats, the bedrock will slowly rebound because of the smaller weight on the surface. This will initially cause a series of big inland lakes to appear below sea level. After 3000 years, almost all the initial depressed areas will have risen above sea level again. Such a complete melting of the Greenland ice sheet is predicted to produce a rise in sea level of about 7m.

The melting in Antarctica will be much smaller and slower even than that in Greenland, because of the size of the ice sheet and the very cold temperatures there at present. However, some regions of East Antarctica may experience a significant melting on similar timescales to those of Greenland.

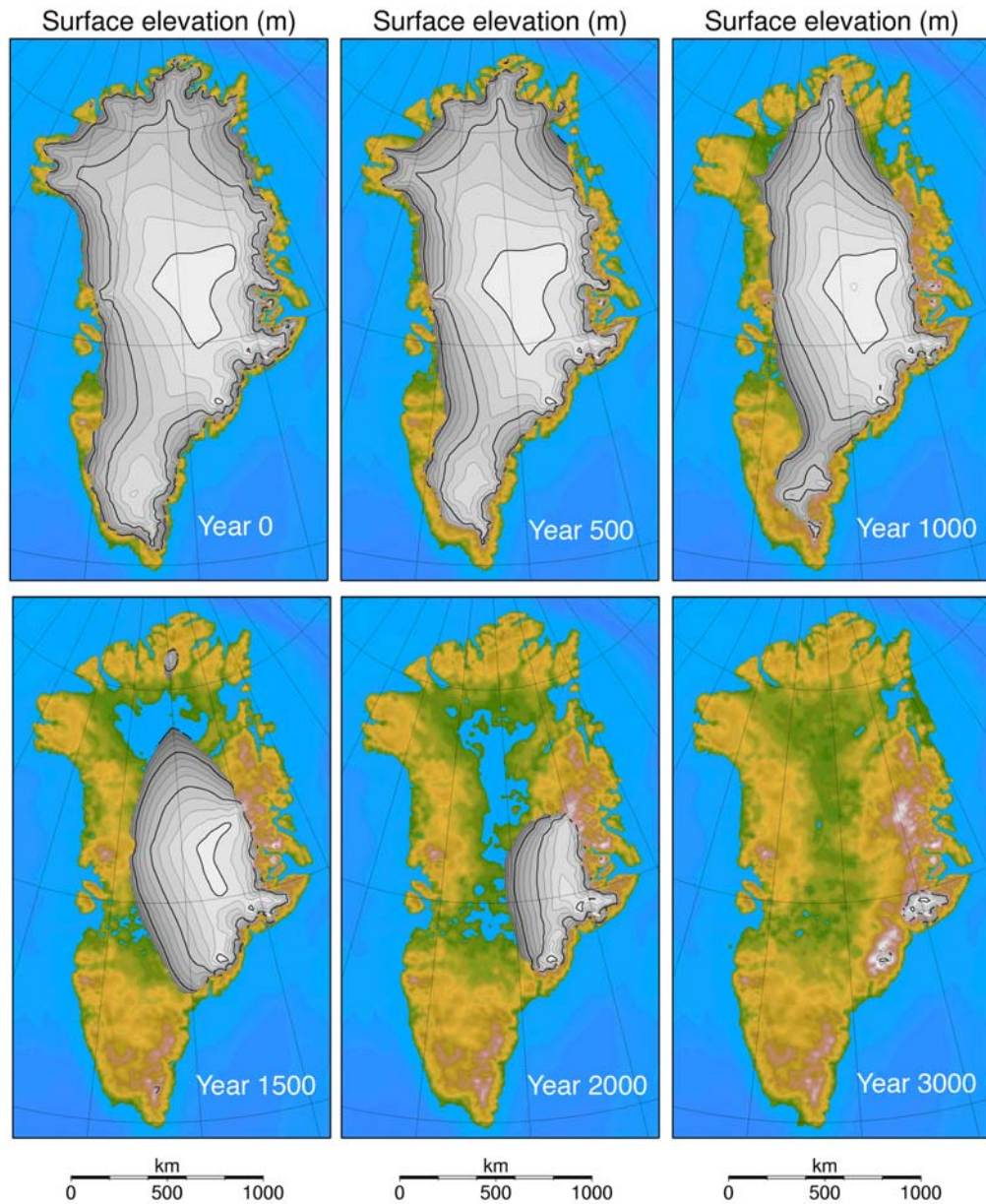


Figure 6.21: Snapshots of the changes in the Greenland ice sheet in a scenario in which the CO_2 concentration is maintained at four times the pre-industrial value (4-times CO_2 scenario) for 3000 years. The results come from the intermediate-complexity climate model LOVECLIM, and show the conditions at the present land surface. The sea and land below sea level is shown in blue, ice-free tundra in brown and green, and the ice sheet in grey. The contour intervals over the ice are 250 m, with thick lines at 1000 intervals (Fichefet et al., 2007).

Cited references and further reading

Archer D. and V. Brovkin (2008). The millennial atmospheric lifetime of anthropogenic CO₂ Climatic Change 90, 283-297.

Bindoff, N.L., J. Willebrand, V. Artale, A. Cazenave, J. Gregory, S. Gulev, K. Hanawa, C. Le Quéré, S. Levitus, Y. Nojiri, C.K. Shum, L.D. Talley and A. Unnikrishnan, (2007). Observations: Oceanic Climate Change and Sea Level. In: Climate Change 2007: The Physical Science Basis. Contribution of Working Group I to the Fourth Assessment Report of the Intergovernmental Panel on Climate Change [Solomon, S., D. Qin, M. Manning, Z. Chen, M. Marquis, K.B. Averyt, M. Tignor and H.L. Miller (eds.)]. Cambridge University Press, Cambridge, United Kingdom and New York, NY, USA. (www.ipcc.ch).

Cadule P., L. Bopp, and P. Friedlingstein (2009). A revised estimate of the processes contributing to global warming due to climate-carbon feedback. Geophys. Res. Lett. 36, L14705, doi:10.1029/2009GL038681

Fichefet, T., E. Driesschaert, H. Goosse, P. Huybrechts, I. Janssens, A. Mouchet, and G. Munhoven, 2007: Modelling the evolution of climate and sea level during the next millennium (MILMO). Scientific Support Plan for a Sustainable Development Policy, SPSD II, Part 2: Global Change, Ecosystems and Biodiversity, Atmosphere and Climate, Belgian Science Policy, Brussels, 131 pp.

Friedlingstein P., P. Cox, R. Betts, L. Bopp, W. Von Bloh, V. Brovkin, P. Cadule, S. Doney, M. Eby, I. Fung, G. Bala, J. John, C. Jones, F. Joos, T. Kato, M. Kawamiya, W. Knorr, K. Lindsay, H. D. Matthews, T. Raddatz, P. Rayner, C. Reick, E. Roeckner, K.-G. Schnitzler, R. Schnur, K. Strassmann, A. J. Weaver, C. Yoshikawa, and N. Zeng (2006). Climate-carbon cycle feedback analysis: results from the C4MIP model intercomparison. Journal of Climate, 19, 3337, 3353.

Hawkins E. and R. Sutton (2009). The potential to narrow uncertainty in regional climate predictions', Bulletin of the American Meteorological Society, 90, 1095-1107 (<http://journals.ametsoc.org/doi/abs/10.1175/2009BAMS2607.1>).

Meehl, G.A., T.F. Stocker, W.D. Collins, P. Friedlingstein, A.T. Gaye, J.M. Gregory, A. Kitoh, R. Knutti, J.M. Murphy, A. Noda, S.C.B. Raper, I.G. Watterson, A.J. Weaver and Z.-C. Zhao, 2007: Global Climate Projections. In: Climate Change 2007: The Physical Science Basis. Contribution of Working Group I to the Fourth Assessment Report of the Intergovernmental Panel on Climate Change [Solomon, S., D. Qin, M. Manning, Z. Chen, M. Marquis, K.B. Averyt, M. Tignor and H.L. Miller (eds.)]. Cambridge University Press, Cambridge, United Kingdom and New York, NY, USA. (www.ipcc.ch).

Moss R., M. Babiker, S. Brinkman, E. Calvo, T. Carter, J. Edmonds, I. Elgizouli, S. Emori, L. Erda, K. Hibbard, R. Jones, M. Kainuma, J. Kelleher, J.-F. Lamarque, M. Manning, B. Matthews, J. Meehl, L. Meyer, J. Mitchell, N. Nakicenovic, B. O'Neill, R. Pichs, K. Riahi, S. Rose, P. Runci, R. Stouffer, D. van Vuuren, J. Weyant, T. Wilbanks, J. P. van Ypersele, M. Zurek (2007). Towards new scenarios for analysis of emissions, climate change, impacts, and response strategies, IPCC expert meeting report, 19–21 September, 2007, Noordwijkerhout, The Netherlands, 166 pp. (<http://www.ames.ucar.edu/docs/IPCC.meetingreport.final.pdf>).

Moss R.H., J. A. Edmonds, K. A. Hibbard, M. R. Manning, S. K. Rose, D. van Vuuren, T. R. Carter, S. Emori, M. Kainuma, T. Kram, G. A. Meehl, J. F. B. Mitchell, N.

Nakicenovic, K. Riahi, S. J. Smith, R. J. Stouffer and A. M. Thomson (2010). The next generation of scenarios for climate change research and assessment. *Nature* 463, 747-756.

Nakicenovic N. and R. Swart (eds.) (2000). IPCC Special report on emission scenarios Cambridge University Press, UK. pp 570 (<http://www.ipcc.ch/ipccreports/sres/emission/index.php?idp=0>).

Solomon, S., D. Qin, M. Manning, R.B. Alley, T. Berntsen, N.L. Bindoff, Z. Chen, A. Chidthaisong, J.M. Gregory, G.C. Hegerl, M. Heimann, B. Hewitson, B.J. Hoskins, F. Joos, J. Jouzel, V. Kattsov, U. Lohmann, T. Matsuno, M. Molina, N. Nicholls, J. Overpeck, G. Raga, V. Ramaswamy, J. Ren, M. Rusticucci, R. Somerville, T.F. Stocker, P. Whetton, R.A. Wood and D. Wratt, 2007: Technical Summary. In: *Climate Change 2007: The Physical Science Basis. Contribution of Working Group I to the Fourth Assessment Report of the Intergovernmental Panel on Climate Change* [Solomon, S., D. Qin, M. Manning, Z. Chen, M. Marquis, K.B. Averyt, M. Tignor and H.L. Miller (eds.)]. Cambridge University Press, Cambridge, United Kingdom and New York, NY, USA.

Vermeer M. and S. Rahmstorf, 2009. Global sea level linked to global temperature. *Proceedings of the National Academy of Sciences*, 106 21527-21532 (<http://www.pnas.org/content/106/51/21527>)

Exercises

Exercises are available on the textbook website (<http://www.climate.be/textbook>) and on iCampus for registered students.

Web links

RCP Database <http://www.iiasa.ac.at/web-apps/tnt/RcpDb/dsd?Action=htmlpage&page=welcome#intro>